Electronic Supplementary Material (ESI) for Lab on a Chip.

Supplementary Information

Capacitive platform for real-time wireless monitoring of liquid wicking in a paper strip

Isidoro Ruiz-García[a,b,d], Pablo Escobedo[a,b,d], Celia E. Ramos-Lorente[b,c], Miguel M. Erenas[b,c], Luis F. Capitán-Vallvey[b,c], Miguel A. Carvajal[a,b,d], Alberto J. Palma[a,b,d,*], Nuria López-Ruiz[a,b,d]

[a] *Electronic and Chemical Sensing Solutions (ECsens), CITIC-UGR, Department of Electronics and Computer Technology, University of Granada (UGR), 18071 Granada, Spain.*

[b] *Unit of Excellence in Chemistry Applied to Biomedicine and the Environment of the University of Granada, Granada, Spain.*

[c] *Electronic and Chemical Sensing Solutions (ECsens), Department of Analytical Chemistry, University of Granada (UGR), 18071 Granada, Spain.*

[d] *Sport and Health University Research Institute (iMUDS), University of Granada (UGR), 18071 Granada, Spain*

Measurement procedure and smartphone application

The procedure for measuring capacitance as a function of time, $\Delta C_{exp}(t)$, is illustrated in the flow diagram presented in Figure S1.

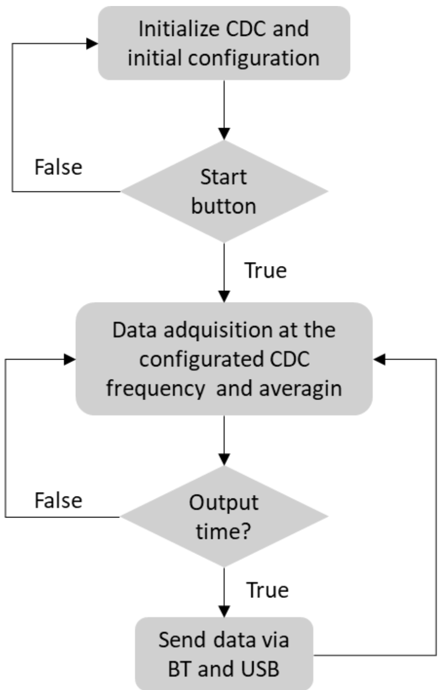

Figure S1. Flow chart of the measurement procedure of the capacitance

A customized smartphone application was developed to enable easy connection and data reception from the capacitive sensing platform, as illustrated in Figure S2. Upon the first opening of the application, the user must conduct the pairing process with the Bluetooth device, which can be done using the 'Discover' button to select the sensing platform from a list of available devices. Once paired, the application automatically saves the device's MAC address in a plain text file on the internal memory of the smartphone. In this way, whenever the user opens the application, they can simply click on the 'Connect' button to automatically bond with the sensing platform without requiring another pairing process since the keys have been already established. Once connected, the user only needs to press the 'Start' button on the screen to activate the reception mode. After this, when the user clicks on the physical start button on the sensing platform (refer to Figure 2c), the application begins to receive and graph the data in real-time via the Bluetooth connection. After the completion of the data acquisition process, the user can navigate through the graphed data and select specific data points by using pinch and zoom gestures. Additionally, the application features an action bar, as shown in Figure S2, with several options that allow the user to save the acquired data (both numeric data and graph) on the smartphone's internal memory, clear the chart for new data acquisition, or share the results through email and various cloud or messaging services. A video demonstration of the smartphone application working in connection with the capacitive sensing platform is available in the Supplementary Movie.

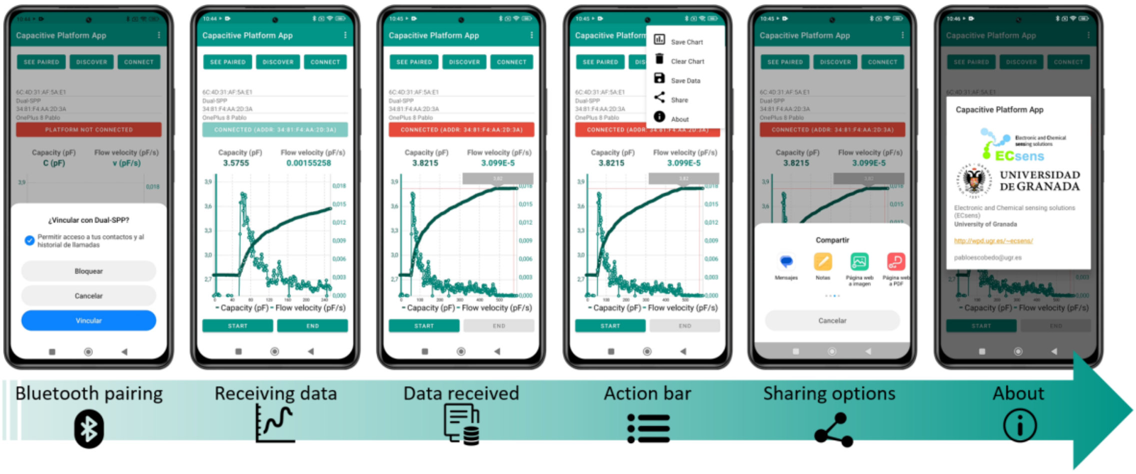

Figure S2. Smartphone app screenshots illustrating some of the key steps of the connection with the capacitive sensing platform, including pairing, data reception, and available options.

Numerical analysis

To demonstrate the impact of including the pore size reduction, α, resulting from paper swelling on the flow dynamics, Figure S3 shows the absorbed water mass for a range of α values from 0 to $2\cdot10^{-3}$ s^{-1}.

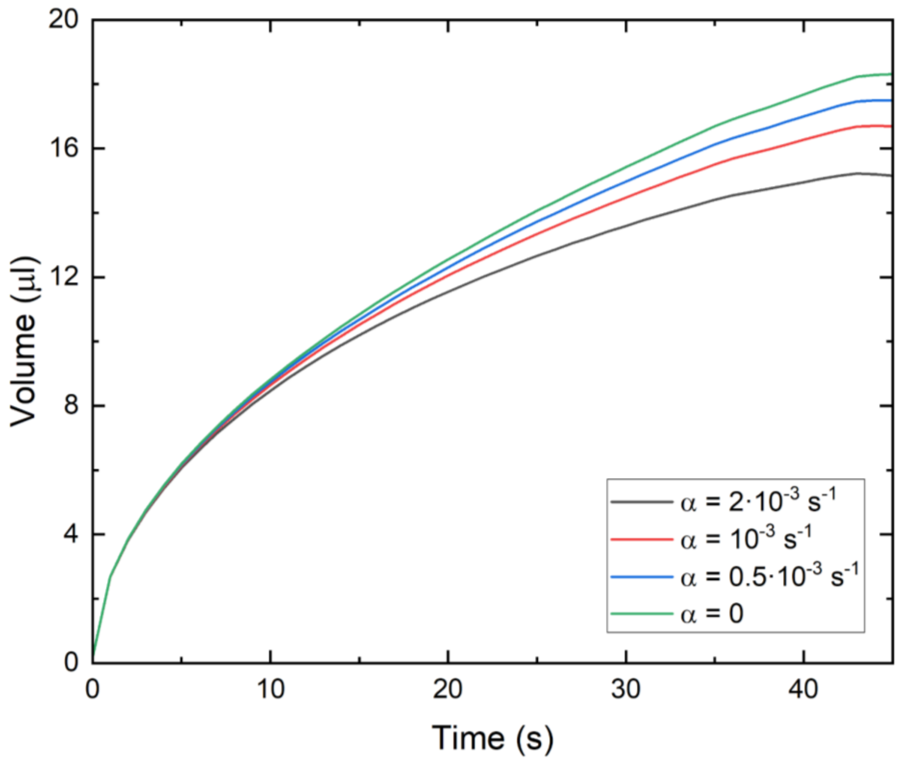

Figure S3. Simulated water intake vs time for various pore size reduction coefficients, α. Geometry of the paper strip is, as validation and reproducibility tests, described in the experimental setups.

A study on the sensitivity of the flow parameters (intake volume, *v*, and flow rate, *FR*) to variations in paper properties was conducted. The classical definition of relative sensitivity between parameter *y* with variations in parameter *x* (S_y^x) is considered as follows:

$$S_y^x = \frac{\Delta y}{\Delta x},$$

where variations of *y* and *x* are considered as normalized variations.

Separate simulations were performed for initial porosities (ε_{p0}) of 0.6, 0.66, and 0.72; wet paper thicknesses (th_w) of 210, 230, and 250 µm; and initial permeabilities (k_0) of $4.0\cdot10^{-13}$, $4.4\cdot10^{-13}$, and $4.8\cdot10^{-13}$ m^2. These curves are depicted in Figure S4. Based on these results, the normalized sensitivities were calculated:

$$S_v^{\varepsilon_{p0}} = S_{FR}^{\varepsilon_{p0}} = S_v^{th_w} = S_{FR}^{th_w} = 1$$

$$S_v^{k_0} = 0.4, \quad S_{RF}^{k_0} = 0.11$$

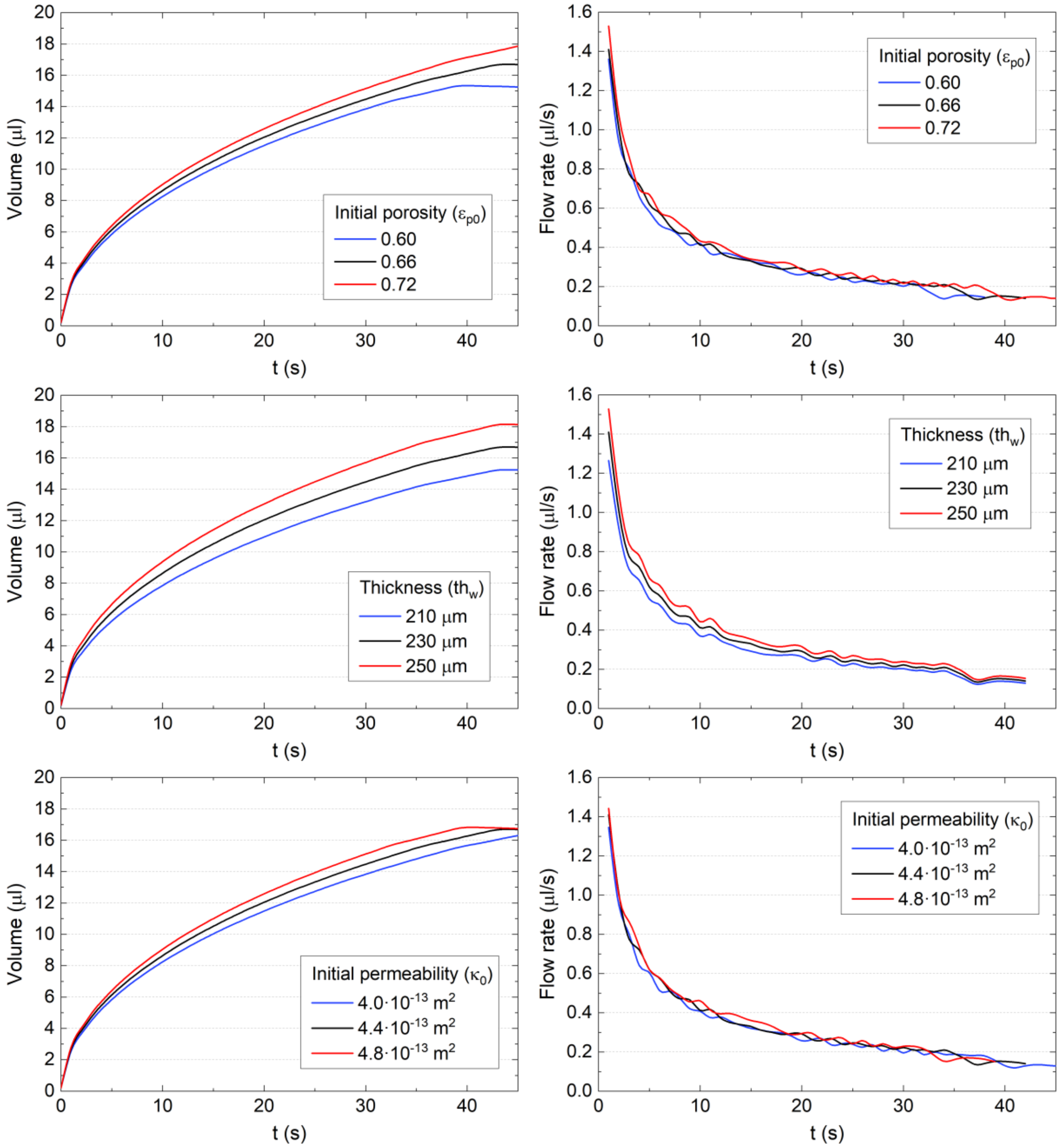

Figure S4. Simulated wicking dynamics (i.e., volume variation and flow rate) over time with varying initial porosity, wet paper thickness, and initial permeability.